Vacancy– and acceptor–H complexes in InP

C P Ewels†, S Öberg‡, R Jones†, B Pajot§ and P R Briddon∥

† Department of Physics, University of Exeter, Exeter EX4 4QL, UK
‡ Department of Mathematics, University of Luleå, Luleå, S95187, Sweden
§ Groupe de Physique des Solides, Universite Paris VII, 2 place Jussieu, 75251 Paris Cédex 05, France
∥ Department of Physics, University of Newcastle, Newcastle NE1 7RU, UK

Abstract. It has been suggested that iron in InP is compensated by a donor, related to the 2316 cm^{-1} local vibrational mode and previously assigned to the fully hydrogenated indium vacancy, $V_{In}H_4$. Using AIMPRO, an *ab initio* local density functional cluster code, we find that $V_{In}H_4$ acts as a single shallow donor. It has a triplet vibrational mode at around this value, consistent with this assignment. We also analyse the other hydrogenated vacancies $V_{In}H_n$, $n = 1, 3$, and determine their structure, vibrational modes, and charge states. Substitutional group II impurities also act as acceptors in InP, but can be passivated by hydrogen. We investigate the passivation of beryllium by hydrogen and find that the hydrogen sits at a bond-centred site and is bonded to its phosphorus neighbour. Its calculated vibrational modes are in good agreement with experiment.

1. Introduction

There is great interest in the electrical effects associated with heavy iron doping of InP. Iron doping is used to produce mid-gap levels, allowing the use of InP as a semi-insulating substrate [1, 2]. However, Fe has many unusual properties in InP which are not yet fully understood. In particular, the charge compensation mechanism of iron has not yet been fully explained [3].

It is known that in InP:Fe, the Fe substitutes for In and primarily adopts the neutral Fe_{In}^{3+} state (labelled 3+ to denote its oxidation state). However, some of the iron is compensated, forming Fe_{In}^{2+}, and metallic donor defects are not present in sufficiently high concentrations to account for this. Therefore it has been proposed that another donor must be present; however, its identity is not established. Recent work has shown a correlation between the intensity of the 2316 cm^{-1} LVM and the Fe_{In}^{3+} concentration [3], suggesting that this defect could be the unknown donor.

When InP is grown by the LEC method using wet boric oxide as the encapsulant, the water vapour dissociates and hydrogen is incorporated into the material. The most intense H-related mode in as-grown crystals occurs at 2316 cm^{-1} (found in InP:Fe as well as in crystals without Fe), and has been associated with $V_{In}H_4$ [4].

This assignment has been made for several reasons. Uniaxial stress measurements show the centre to have T_d symmetry [4], consistently with $V_{In}H_4$. The LVM lies close to that of other P–H-related modes, and this is consistent with results obtained for VH_4 in Si [5]. The defect can be created by proton irradiation [6], which also leads to the creation of the required In vacancies.

H/D mixed defects have not been observed on mixed H^+/D^+ implantation because the signal-to-noise ratio of published spectra [6] is not high enough, and the FWHPs of the proton- and deuteron-induced LVMs are too broad for the individual components to be resolvable. This last point is probably the origin of the apparent decrease in intensity of the 2316 cm^{-1} line reported for mixed implantation, since there are several components near 2316 cm^{-1}. The inverse is observed for the LVM at 2202 cm^{-1} assigned to $V_{In}H$, and this contrasting result also supports the assignment.

Other LVMs in SI InP include H–acceptor modes (mainly (Zn, H)) due to inadvertent contamination, as well as other LVMs whose origin is not clear. In slightly n-type InP:Fe, the (Zn, H) LVM is not observed, but another LVM at 2285 cm^{-1} is always observed. Annealing of LEC InP produces LVMs attributed to partially hydrogenated vacancies, but these are much lower in intensity than the line at 2316 cm^{-1}.

There has been no theoretical examination of these defects performed to date. We therefore investigate the structure, local vibrational modes and charge states of a range of hydrogenated vacancies, $V_{In}H_n$, $n = 0, 4$.

Group II residual impurities are normally present in InP at low concentrations. They are known to act as acceptors, producing shallow levels in the gap [7]. It has been observed that the presence of hydrogen is able to passivate these impurities, and it is only recently that there have been attempts to fully understand this process [4, 8].

Experimental investigations of H- and D-plasma-passivated Be, Mg, Cd and Zn have been performed [4].

Infrared absorption studies show hydrogen local vibrational modes (LVMs) which lie in the frequency range where P–H stretch modes are expected ($\approx$2200–2300 cm^{-1}). This suggests that hydrogen bonds to phosphorus atoms in the lattice instead of the acceptor impurities.

Uniaxial stress measurements show that these acceptor–hydrogen defects have C_{3v} symmetry [4]. Therefore, since these group II acceptors are known to substitute for indium, hydrogen must lie somewhere along the $\langle 111 \rangle$ acceptor–P direction. Passivation with a mixed H, D plasma produces no peak splitting, suggesting that there is only one hydrogen atom present in each defect. It was suggested that passivation occurred through a chemical recombination, allowing a lower coordination for the group II acceptor atoms and tying up the resultant dangling bond on the neighbouring phosphorus atom [4].

We examine several possible Be–H complexes in InP in order to determine the lowest-energy structure and the passivation mechanism of the hydrogen.

2. Method

The calculations used here are *ab initio* local density functional pseudopotential ones carried out on large H-terminated clusters using the serial version of the AIMPRO code (described in detail elsewhere [9]). The electronic wavefunctions are expanded in s and p Gaussian orbitals centred at nuclei as well as at bond centres. Norm-conserving pseudopotentials [10] are used in order to exclude core electrons. The self-consistent energy E and the force on each atom are calculated and the atoms moved by a conjugate gradient algorithm to equilibrium.

Throughout this paper, a fixed notation is used to indicate the basis sets used to model each atom type. Each atom requires a number of Gaussian basis functions for the wavefunction and charge density. $A(n, m)$ indicates that for atom type A we used n wavefunction basis functions and m charge-density basis functions. In the text we describe additional Gaussian basis functions which are placed on bond centres to allow more accurate modelling. These basis functions make it unnecessary to include d orbitals sited at the In atomic sites.

Initial calculations on pure InP used an 86-atom bond centred cluster, $In_{22}P_{22}H_{42}$ with C_{3v} symmetry. We fitted a Musgrave–Pople interatomic potential to the pure InP dynamical matrix and used this to determine the bulk phonon modes. The basis sets used were $In(8, 8)$, $P(8, 8)$ and $H(2, 3)$, with bond-centred fitting functions on all of the bonds between the inner eight atoms. Symmetry was maintained at C_{3v} throughout.

In order to examine the hydrogenated vacancies, we generated a 131-atom hydrogen-terminated InP cluster, $In_{31}P_{40}H_{60}$. The central In atom was replaced by up to four hydrogen atoms (see figure 1). Symmetry was only enforced for $V_{In}H_4^+$ (T_d). Two electrons were added for each bond, so the resultant cluster charge was $+9$. In order to keep the cluster charge constant, the structures optimized were $V_{In}H_4^+$, $V_{In}H_3$, $V_{In}H_2^-$, $V_{In}H^{2-}$ and V_{In}^{3-}. The electronic spin component was averaged.
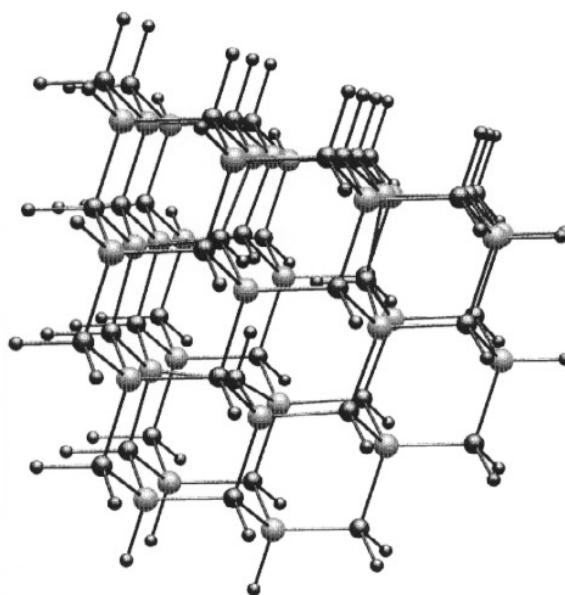
Figure 1. The 134-atom cluster $In_{30}P_{40}H_{64}$ containing the defect $V_{In}H_4^+$.

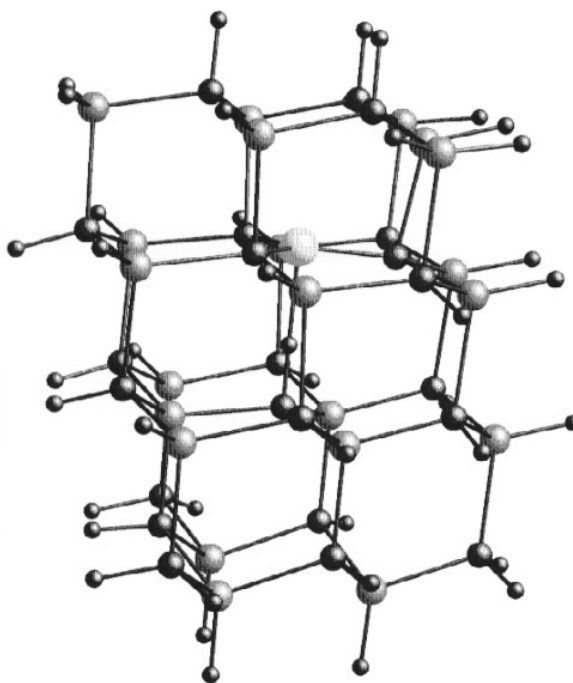**Figure 2.** The 88-atom cluster $BeIn_{21}P_{22}H_{43}$.

The basis sets used were $In(8, 8)$, $P(4, 5)$ and $H(2, 3)$. Bond-centred Gaussians were placed on the twelve In–P bonds neighbouring the vacancy.

For examination of the Be–H complexes we generated an 86-atom hydrogen-terminated InP cluster, $In_{22}P_{22}H_{42}$. This is In–P bond centred. The centre In atom was replaced with Be, and a H atom inserted at one of three different sites: antibonded behind the Be, antibonded behind the P, and in the bond centre between Be and P. This resulted

Table 1. Phonon frequencies for pure InP (cm^{-1}).

Location	Mode	Neutron diffraction (300 K) [15]	Raman scattering (300 K) [16]	Far IR (20 K) [12]	Theoretical
$\Gamma(0,0,0)$	LO		345.4	351	354.80
	TO	307 ± 7	303.3		354.80
$X(1,0,0)$	LO	332 ± 3		328.5	324.59
	TO	324 ± 7		326.5	317.46
	LA	194 ± 10		190.5	186.86
	TA	68 ± 3		67.5	69.59
$L(\frac{1}{2},\frac{1}{2},\frac{1}{2})$	LO	340 ± 10		340.5	335.27 (5, 6)
	TO	317 ± 5		315.5	314.03 (4)
	LA	167 ± 3		167.5	171.19
	TA	55.0 ± 0.7		53.5	49.49

in the cluster $BeIn_{21}P_{22}H_{43}$ (see figure 2). Symmetry was constrained to be C_{3v}. The basis sets used were $In(8,8)$ and $P(8,8)$ for the seven core InP atoms, $In(4,5)$ and $P(4,5)$ for the rest, $Be(6,6)$ and $H(3,4)$. Bond-centred Gaussians were placed between the inner nine atoms.

The eigenvalues calculated here are Kohn–Sham eigenvalues, and are not directly comparable with experimental eigenvalues. LDF theory tends to underpredict bandgaps, whereas finite cluster sizes broaden them. Thus these calculated eigenvalues indicate qualitatively whether defect levels lie in the gap, but are only quantitatively useful when comparing similar clusters.

3. Pure InP

Initial investigations centred on pure InP, in order to determine vibrational frequencies and a phonon dispersion curve, and to obtain a set of Musgrave–Pople interatomic potentials for frequency calculations in the defect clusters.

After relaxation, we obtained central InP bond lengths of 2.480 Å along the $\langle 111 \rangle$ axis parallel to the C_{3v} axis, and 2.421 Å otherwise (errors of 2.4% and 4.7% respectively, as the experimental bond length is 2.54 Å [11]). The bond elongation in the (111) direction is due to the intrinsic dipole moment of a bond-centred cluster. The nearest-neighbour P–In–P bond angle was 111.5°, and 107.3° when using the In–P bond parallel to the C_{3v} axis; these are within 2° of the tetrahedral angle.

A supercell calculation of the full phonon dispersion curve was performed using the Musgrave–Pople interatomic potential. This is given in figure 3 along with various experimental values. Selected values from this curve are given in table 1. We do not obtain any LO–TO splitting because of an absence of long-range electric field effects in the potential. The highest bulk phonon modes are 354.80 (351), 324.59 (328.5), and 335.27 cm^{-1} (340.5 cm^{-1}) at Γ, X, and L respectively (the experimental modes at 20 K are in brackets [12]); thus our frequency errors are ≈ 4 cm^{-1}. The calculated bandgap for InP was 0.84 eV, compared to an experimental value of 1.34 eV deduced from optical data [13], and is in good agreement with a previous LDF value of 0.8 eV [14] (see section 2 above). Our calculated
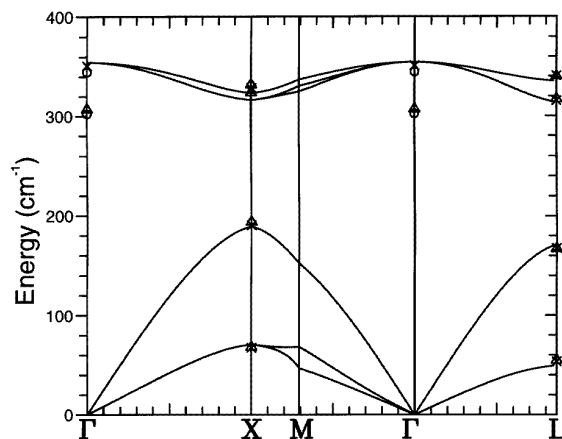
Figure 3. The calculated phonon dispersion curve for InP.

Table 2. Calculated LVMs for the fully hydrogenated vacancy in InP, $V_{In}H_nD_m^+$, $n + m = 4$. The asterisk indicates IR inactive; T indicates triplet and D, doublet.

H$_4$	H$_3$D	H$_2$D$_2$	HD$_3$	D$_4$
2387.85 *	2380.18	2372.34	2364.31	1713.01 *
2356.40 T	2356.32 D	2356.24	1707.26	1690.82 T
618.57 D	1696.43	1701.74	1690.95 D	445.34 D
565.87 T	603.12 D	1691.08	549.65 D	411.94 T
408.69 T	565.71	595.02	428.92 D	
	508.72 D	556.04	412.03	
	408.69	541.80		
		481.28		
		425.83		

bandgap is underestimated, which is unusual for a cluster calculation.

We conclude that our method gives bond lengths and local vibrational modes within an acceptable error range.

4. Hydrogenated vacancy centres

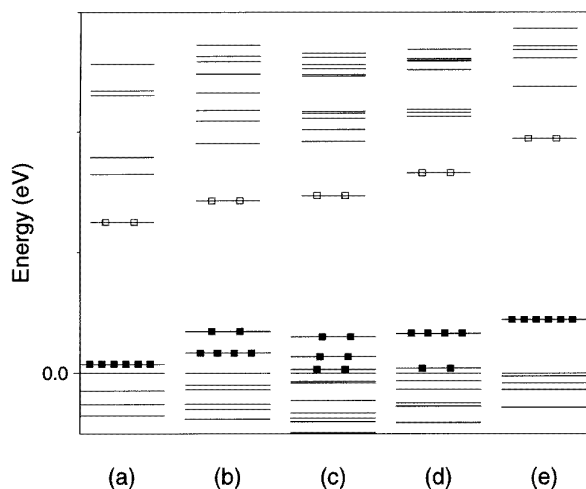The local vibrational modes for $V_{In}H_4$ with pure and mixed isotope compositions are shown in table 2. The highest

Figure 4. The top Kohn–Sham eigenvalues of the hydrogenated vacancies; (a) $V_{In}H_4^+$, (b) $V_{In}H_3$, (c) $V_{In}H_2^-$, (d) $V_{In}H^{2-}$, (e) V_{In}^{3-}. Filled boxes indicate electrons and empty boxes indicate holes. The eigenvalues have been arbitrarily shifted to align the highest filled level below the t_2-like state with zero.

IR visible mode for $V_{In}H_4^+$ at 2356.4 cm^{-1} is in excellent agreement with experiment (2315.6 cm^{-1}, a 1.8% error), as is the 1690.8 cm^{-1} mode for $V_{In}D_4^+$ (experimental value of 1683.4 cm^{-1}, an error of 0.4%). This small drop in error with deuteration suggests only limited anharmonic character in the bonding [17].

The LVMs for the range of hydrogenated vacancies, $V_{In}H_n$, $n = 0, 4$, are shown in table 3. The results show that as the number of H atoms in the vacancy increases, the P–H bonds are shortened and the frequency of the vibrational modes increases. This is due to the compressive effect of the other hydrogen atoms on each P–H group, coupled with the removal of dangling bonds from 'unsaturated' P atoms which would have acted to attract the hydrogen away from its phosphorus neighbour. This is consistent with previous results obtained for Si [5, 18].

The shift in P–H length from $V_{In}H_4$ to $V_{In}H$ is only 2.1% (from 1.419 Å to 1.450 Å), but it leads to a 9.9% shift in vibrational mode (2387.8 cm^{-1} to 2150.7 cm^{-1}). The calculated H stretch modes of the partially hydrogenated vacancies could account for a group of experimentally observed vibrational modes lying between 2200 and 2290 cm^{-1} [4, 19].

The top Kohn–Sham eigenvalues of the hydrogenated vacancies are shown in figure 4. In each case there is a t_2-like state above the top of the valence band which splits as the number of H atoms decreases, and a singlet state near to the conduction band. In the fully hydrogenated neutral vacancy, $V_{In}H_4$, the singlet is partially occupied, and therefore acts as a donor.

As each hydrogen atom is removed from the vacancy, an electron is removed from the highest occupied state. The resulting defects can act as acceptors that fill the t_2 level when ionized. This level is already filled in the case of $V_{In}H_3$ so this defect cannot act as an acceptor. However, $V_{In}H_2$, $V_{In}H$ and V_{In} will behave as single, double and triple acceptors respectively.
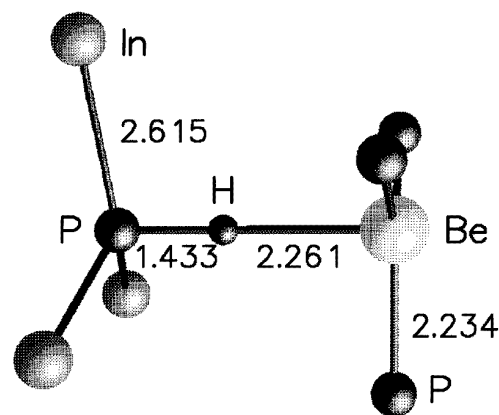

Figure 5. The calculated structure for H-passivated Be in InP (the bond lengths are in Å).

The t_2 level is split due to the lower symmetry of the partially hydrogenated vacancies. $V_{In}H_4^+$ has T_d symmetry and therefore the level does not split. $V_{In}H_3$ has C_{3v} symmetry, so the t_2 level splits into an e and an a_1 level. $V_{In}H_2^-$ has C_{2v} symmetry which leads to three separated singlets. $V_{In}H^{2-}$ and V_{In}^{3-} are directly comparable with $V_{In}H_3$ and $V_{In}H_4^+$, with the dangling and hydrogen-terminated bonds reversed, in addition to the a–e level ordering. This t_2-like state gradually moves upwards away from the valence band as hydrogen atoms are removed. In V_{In}^{3-} the t_2 level is quite deep in the gap.

The indium vacancy, V_{In}^{3-}, fits the trend of increasing acceptor character with a decreasing number of hydrogen atoms present. Previous calculations [20] also show V_{In} to be a triple acceptor.

High-temperature annealing of InP:Fe reduces the concentration of $V_{In}H_4^+$. This is due to the partial dissociation of this centre and, up until now, only $V_{In}H$ has been identified with certainty. It is shown here that $V_{In}H_2$ and $V_{In}H$ are acceptors. In annealed high-resistivity material they should cause a drop in the Fe^{2+} concentration. This will be in addition to the decrease in concentration of Fe^{2+} due to loss of the $V_{In}H_4$ donor.

In contrast, von Bardeleben *et al* [21] found that thermal annealing of Fe-doped InP in the range 660–820 °C led to an increase in Fe^{2+} concentration. They suggested that this was due to the formation of some unidentified deep thermal donors. This could be associated with other hydrogen complexes. However, from this work it seems unlikely that hydrogenated vacancies are responsible.

In summary, the fully hydrogenated vacancy, $V_{In}H_4$, acts as a single donor due to a partially filled singlet near the top of the gap; thus $V_{In}H_4$ will compensate Fe$_{In}^{3+}$ in InP. Removal of hydrogen atoms from the vacancy leads to increased acceptor character as the triplet state starts to empty.

5. Passivation of group II impurities

Be was used to determine the preferential site for hydrogen in the passivated group II acceptor–hydrogen complex. In order to maintain C_{3v} symmetry along the (111) axis,

Table 3. The local vibrational modes (cm^{-1}), symmetry, and calculated bond lengths (Å) of hydrogenated vacancies in InP. The asterisk indicates IR inactive; T indicates triplet and D, doublet.

| Defect | Local vibrational modes | | | | | Symmetry | Bond length |
	Experiment [6]	[4] ([19])	Calculation				
$V_{In}H_4^+$	2315.2	2315.6	2387.8 *	2356.4 T	618.6 D	T_d	1.419
$V_{In}D_4^+$	1683.4		1713.0 *	1690.8 T	445.3 D		
$V_{In}H_3$			2324.1	2286.3 D	695.3 D	C_{3v}	1.429
$V_{In}D_3$			1667.6	1640.8 D	498.2 D		
$V_{In}H_2^-$			2256.2	2216.8	730.0	C_{2v}	1.439
			617.7	611.8	602.0		
$V_{In}D_2^-$			1619.4	1591.6	523.0		
			446.4	444.4	438.8		
$V_{In}H^{2-}$	2201.7	(2202.4)	2150.7	644.9	644.7	C_{3v}	1.450
$V_{In}D^{2-}$	1603.8		1544.7	467.5	467.4		

Table 4. Calculated and experimental LVMs for H-passivated Be in InP (cm^{-1}).

| Experimental | | Bond centred | | Antibonded behind P | |
H	D	H	D	H	D
2236.5	1630.9	2287.71	1639.90	2469.85	1770.94

hydrogen can sit at one of only three sites: at the P–Be bond centre, or one of the two antibonded sites behind P or Be (see figure 5).

The structure with H lying in an antibonded site behind Be was 1.77 eV higher in energy than in the bond-centred case, and so was energetically unfavourable. The structure with H antibonded behind P was only 0.13 eV higher in energy than the bond-centred case, close to the expected errors in our calculation. In all cases the gap was cleared of any acceptor levels by the presence of the hydrogen atom, showing that it has passivated the acceptor activity. In order to determine whether the bond-centred or 'antibonded behind P' model is correct, it is necessary to examine the LVMs, shown in table 4.

As can be seen, the calculated LVMs for the bond-centred case are in good agreement with experiment (errors of 2.3% and 0.6% for H and D respectively) whereas the results from antibonding are poor (10.4% and 8.6% for H and D respectively). From this we conclude that the preferential H site is at the bond-centred location.

The defect is shown in figure 5. The large H–Be separation shows a lack of bonding between H and Be; the H atom is strongly bonded to P. The P–H bond length is comparable to the P–H bond lengths in the hydrogenated vacancy, and compares to an experimental bond length for the P–H$_3$ molecule of 1.43 Å [11]. The Be–P bond lengths are similar to crystalline Be–P lengths in Be$_3$P$_2$ (2.16 Å). The impurity is displaced along the $\langle 111 \rangle$ direction away from the hydrogen atom to achieve this, until it is coplanar with the phosphorus atoms.

Therefore we conclude that substitutional Be acceptors are passivated by a single H sitting at a bond-centred position between the Be atom and a nearest-neighbour P atom. We find a LVM at 2287.71 cm^{-1}, 2.3% larger than the experimental frequency. There is also an undetected wag mode at 644 cm^{-1}, similar to that of the C–H defect

in GaAs and AlAs [17, 22]. Work is currently under way to determine whether this behaviour is typical of other group II acceptor atoms in InP.

6. Conclusions

Our conclusions are as follows.

(1) Our LDF calculations predict the highest bulk phonon modes in pure InP to be 354.80 (351), 324.59 (328.5), and 335.27 cm^{-1} (340.5 cm^{-1}) at Γ, X, and L respectively (the experimental modes at 20 K are in brackets [12]); thus our frequency errors are 4 cm^{-1}. The error in bond length for pure InP is 4.1%.

(2) $V_{In}H_4$ is shown to be a single donor forming $V_{In}H_4^+$, with a donor level in the upper part of the gap. $V_{In}H_3$ is shown to be electrically inactive, but the partially hydrogenated vacancies, $V_{In}H_2$ and $V_{In}H$, act as acceptors, forming $V_{In}H_2^-$ and $V_{In}H^{2-}$ with acceptor levels in the lower gap region.

(3) $V_{In}H_4$ compensates Fe_{In}^{3+} leading to the formation of Fe_{In}^{2+}. The donor electron could also be trapped by the partially hydrogenated vacancy centres, $V_{In}H_2^-$, and $V_{In}H^{2-}$, or even V_{In}^{3-}; however, these are present in much lower concentrations than is $V_{In}H_4^+$.

(4) The P–H bond length in the hydrogenated vacancy centres becomes shorter as more hydrogen atoms are added to the vacancy. This causes a corresponding increase in the hydrogen local vibrational modes.

(5) The H-related LVMs have been calculated for both the fully and partially hydrogenated vacancies. Darwich *et al* [4] have observed a number of vibrational modes in their InP:Fe samples between 2202.39 cm^{-1} and 2282.8 cm^{-1} which have been attributed to H-related complexes [8], and we suggest that the partially hydrogenated vacancy centres could account for at least some of these modes.

(6) In agreement with experiment, the calculations show that H is able to passivate group II acceptors such as Be. It lies, bond centred, between Be and P, and forms a strong bond with P rather than Be.

(7) H in the bond-centred and two possible antibonding sites (behind P or Be) always passivates the Be atom. However, the antibonding behind Be is 1.77 eV higher in energy than the bond-centred case, and only the bond-centred site produces the correct LVMs. From this we conclude that the H atom must lie bond centred, between Be and P.

(8) The Be moves off-site along the $\langle 111 \rangle$ axis until it lies coplanar with its three P neighbours. This allows it to form stronger, more molecular-like bonds with the P atoms.

Acknowledgments

References

[1] Mizuno O and Watanabe H 1975 *Electron. Lett.* **11** 118
[2] Carnera A, Gasparotto A, Tromby M, Caldironi M, Pellegrino S, Vidimari F, Bocchi C and Frigeri C 1994 *J. Appl. Phys.* **76** 9
[3] Zach F X 1994 *J. Appl. Phys.* **75** 12
[4] Darwich R, Pajot B, Rose B, Robein D, Theys B, Rahbi R, Porte C and Gendron F 1993 *Phys. Rev.* B **48** 24
[5] Bech Neilsen B, Berg Rasmussen F, Hoffmann L, Budde M, Jones R, Goss J and Öberg S 1995 *Mater. Sci. Forum* **196–201** 933–8
[6] Fischer D W, Manasreh M O and Matous G 1992 *J. Appl. Phys.* **71** 4805
[7] Pantelides S T 1975 *Festkörperprobleme (Advances in Solid State Physics)* vol 15, ed P Grosse (New York: Pergamon) p 149
[8] Chevallier J, Clerjaud B and Pajot B 1991 *Hydrogen in Semiconductors* ed J I Pankove and N M Johnson (Orlando, FL: Academic)
[9] Jones R 1992 *Phil. Trans. R. Soc.* A **341** 351
[10] Bachelet G B, Hamann D R and Schlüter M 1982 *Phys. Rev.* B **26** 4199
[11] Slater J 1965 *Quantum Theory of Molecules and Solids* vol 2 (New York: McGraw-Hill)
[12] Koteles E S and Datars W R 1976 *Solid State Commun.* **19** 221
[13] Folberth O G and Weiss H 1955 *Z. Naturf.* a **10** 615
[14] Khowash P K 1994 *Phys. Rev.* B **49** 16
[15] Borcherds P H, Alfrey G F, Saunderson D H and Woods A D B 1975 *J. Phys. C: Solid State Phys.* **8** 2022
[16] Hilsum C, Fray S J and Smith C 1969 *Solid State Commun.* **7** 1057
[17] Jones R, Goss J, Ewels C P and Öberg S 1994 *Phys. Rev.* B **50** 8378
[18] Roberson M A and Estreicher S K 1994 *Phys. Rev.* B **49** 17 040
[19] Clerjaud B, Côte D and Naud C 1987 *Phys. Rev. Lett.* **58** 1755; *J. Cryst. Growth* **83** 190
[20] Seitsonen A P, Virkkunen R, Puska M J and Nieminen R M 1994 *Phys. Rev.* B **49** 5253
[21] von Bardeleben H J, Stievenard D, Kainosho K and Oda O 1991 *J. Appl. Phys.* **70** 7392
[22] Pritchard R, Davidson B R, Newman R C, Bullough T J, Joyce T B, Jones R and Öberg S 1994 *Semicond. Sci. Technol.* **9** 140